



www.ericjournal.ait.ac.th

Hybrid PSO-BP Neural Network Approach for Wind Power Forecasting

Gu Bo^{*1}, Hu Hejuan*, Huang Hui* and Ren Yan*

Abstract –Due to the intermittence and fluctuation of wind power generation, accurate forecasting of wind power is of great significance for the safe and stable operation of wind power integrated system. In the paper, a new wind power forecasting method combining particle swarm optimization (PSO) and back-propagation (BP) neural network is proposed. BP neural network structure was constructed according the number of input data, and PSO algorithm is used to get the optimal initial weights and biases of BP neural network, which can effectively overcome the shortcoming of BP neural network that it is easy to fall into local optimal solution, and increase the convergence speed of BP neural network. Considering the integrity of training data, the PSO-BP neural network was trained to use full year data in 2011. The original BP, PSO-BP, GA-BP and wavelet-BP neural network is applied for 6-h, 1-day, 3-day wind power forecasting in May and December of 2012, respectively. The compared results show that the mean absolute error(MAE) and the root mean square error(RMSE) of wind power forecasting based on PSO-BP neural network are clearly less than that based on original BP, GA-BP and wavelet-BP neural network.

Keywords – BP neural network, numerical weather prediction (NWP), PSO-BP neural network, wind power forecasting, wind power generation.

1. INTRODUCTION

Using non-pollution and renewable energy to replace fossil energy, is one of the future development trends of electric power [1]-[4]. As a kind of renewable energy, wind power is being developed and used on a large-scale. Wind power has the characteristics of random fluctuation and intermittence because of the random fluctuation and intermittence of wind speed, which bring challenges to the stable operation of power grid [5]-[6]. Therefore, it is of great significance to forecast wind power accurately for the safe and stable operation of wind power integrated system.

There have been some studies on wind power forecasting. Based on the time horizon of the forecast, wind power forecasting can be divided into mid-and-long term forecast, short-term forecast and ultra-short-term forecast [7]. Mid-and-long term forecast is mainly used in feasibility study of wind farm design and the forecast of annual power generation after wind farm constructed [8]. Short-term forecast is to facilitate the reasonable dispatch of the power grid and guarantee the quality of the power supply [9]. Ultra-short-term forecast is generally used for wind turbine control [10]-[11].

The methods and techniques for short-term wind power forecast can be categorized as physical methods, statistical methods, hybrid physical-statistical methods. Basically, the statistical methods have been widely studied and applied because of a better prediction accuracy for short-term forecast. The statistical methods include continuous methods, time series methods,

Kalman filtering methods, artificial neural network methods, spatial correlation methods, support vector machine methods and so on. Dennis *et al.* [12] presented an autoregressive model with wavelet decomposition for wind power forecast, and the forecasting results show that the prediction accuracy of the model is significantly improved compared with simple linear prediction model. In view of the disadvantages of gauss regression method, such as computational complexity and non-time varying characteristics, Juan *et al.* [13] presented a gauss forecast model based on time series, and the forecasting results show that this method can reduce the computational complexity and improve the prediction accuracy. The support vector machine based on continuous time segment clustering was proposed for wind power forecasting by [14], and the power output of a certain wind farm was forecasted by this method, the forecasting results show that the method is effective. Aiming at the nonlinear and non-stationary characteristics of wind speed, Hui *et al.* [15] proposed a hybrid wind speed forecast method based on the secondary decomposition algorithm (SDA) and Elman neural networks, and the calculation results show that the hybrid prediction model has satisfactory performance in wind speed forecasting.

The BP neural network was used to forecast short-time wind speed by [16], and the forecasting error was analyzed. The prediction results show that the BP neural network can achieve good results in short-time wind speed forecast. A wind speed forecast method based on kalman and wavelet neural network was proposed by [17], and the prediction results of this method are compared with that of original BP neural network, the compared results show that the proposed algorithm has a higher prediction accuracy. Bonfil *et al.* [18] proposed a wind speed prediction model based on support vector and auto-regressive method, and this prediction model was used to forecast the short-term power output of a

^{*}North China University of Water Resources and Electric Power, School of Electric Power, 36 Beihuan Road, Zhengzhou, Henan, 450045 China.

¹Corresponding author;
E-mail: gb19820915@163.com.

wind farm. The forecasting results show that the prediction accuracy of support vector and auto-regressive method is better than that of auto-regressive model.

Hybrid techniques are proposed with the combination of superior attributes of two or more algorithms, they are widely used in forecasting field. A hybrid intelligent approach named ADE-BPNN is used to estimate energy consumption, and the errors of the test data sets indicate that the ADE-BPNN model can effectively predict energy consumption compared in [19]. The particle swarm optimization back propagation neural network was used the surface ship integrated navigation system of INS/CNS, the results showed that the INS/CNS integrated navigation method based on PSO-BPNN can effectively estimate and compensate the INS navigation error under the star sensor invalid state in [20]. The BP neural network based on particle swarm optimization was used for wind speed forecasting, and the proposed method achieves much better forecast performance than the basic back propagation neural network and ARIMA model in [21]. The PSO-BP network was used in short-term load forecasting, and the calculated results show that the performance prediction of PSO-BP is superior to traditional BP neural network in [22]-[23].

These authors have studied the wind speed forecasting methods and the power forecasting methods, and have gotten some research results. However, due to the stochastic uncertainty of wind speed and the influence of climate and environment, new forecasting methods need to be further explored to improve the prediction accuracy of wind farm power output. Because PSO-BP neural network has a fast convergence speed and strong global search ability, which has been widely used in forecast areas, and its availability has been verified. Therefore, a wind power forecasting method based on particle swarm optimization and back-propagation (PSO-BP) neural network is proposed in the paper. In this method, the BP neural network was constructed according the number of input data, and the initial weights and biases of BP neural network are obtained through the global search ability of particle swarm optimization (PSO) algorithm, and the shortcoming of original BP neural network that is easy to fall into local extremum is effectively solved. The PSO-BP neural network is trained to use the historical data of numerical weather prediction (NWP) and wind power of the year 2011, and then the trained PSO-BP neural network is used to forecast the wind power for 6-h, 1-day, 3-day wind power forecasting in May and December, 2012, respectively. The prediction results of original BP, PSO-BP, GA-BP and wavelet-BP neural network are compared and analyzed.

2. PROPOSED WIND POWER FORECASTING METHOD

The proposed approach is based on a combination of PSO and BP neural network. The PSO is used to determine the initial weights and the biases of BP neural network, which can overcome the shortcoming of BP

neural network that it is easy to fall into local optimal solution.

2.1 BP Neural Network

The learning processes of BP neural network are to constantly adjust the weights and biases, so that the output value of BP neural network is consistent with the target value. The learning processes consist of two processes, including the signal forward propagation and the error back propagation. The learning processes are over when the error of BP network output is reduced to an acceptable level, or the number of iterations reaches the preset value.

BP neural network is generally composed of input layer, hidden layer and output layer. The neurons of the input layer and the hidden layer, the hidden layer and the output layer are connected in one-way connection, respectively. But, there is no connection between the neurons in the same layer. The topology structure of BP neural network is shown as Figure 1.

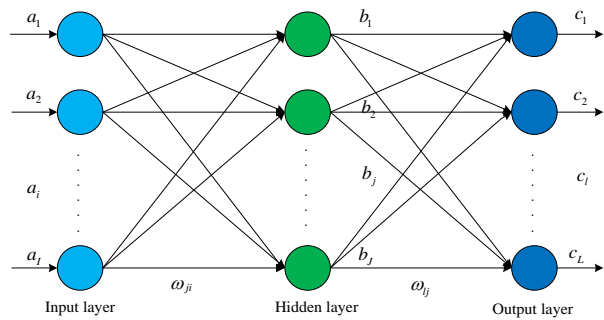


Fig. 1. Structure of BP neural network.

The learning processes of BP neural network are as follows.

A. Calculating the output value of hidden layer neuron.

The output value of hidden layer neuron can be calculated by Equation 1.

$$b_j = f_1 \left(\sum_{i=1}^I \omega_{ji} a_i - \theta_j \right) = f_1 (net_j) \quad (1)$$

Where b_j is the output value of hidden layer neuron; f_1 is the mapping function of hidden layer neuron, which is S-type tangent function; a_i is the input value of input layer neuron; I is the number of input layer neurons; w_{ji} is the connection weight from the input layer neuron i to the hidden layer neuron j ; θ_j is the bias of hidden layer neuron; net_j is the activation value of f_1 .

B. Calculating the output value of output layer neuron

The output value of output layer neuron can be calculated by Equation 2.

$$c_l = f_2 \left(\sum_{j=1}^J \omega_{lj} b_j - \theta_l \right) = f_2 (net_l) \quad (2)$$

Where c_l is the output value of output layer neuron; f_2 is the mapping function of output layer neuron, which is S-type logarithmic function; J is the number of hidden

layer neurons, according to the Kolmogorov theorem, J can be calculated by $J=2I+1$; ω_{lj} is the connection weight from the hidden layer neuron j to the output layer neuron l ; θ_l is the bias of output layer neuron; net_l is the activation value of f_2 .

C. Calculating the overall error value of output layer neurons

The overall error value of output layer neurons can be calculated by Equation 3.

$$\begin{aligned}
 E &= \frac{1}{2} \sum_{i=1}^L [t_i - c_i]^2 \\
 &= \frac{1}{2} \sum_{i=1}^L [t_i - f_2(\sum_{j=1}^J \omega_{lj} b_j - \theta_l)]^2 \\
 &= \frac{1}{2} \sum_{i=1}^L [t_i - f_2(\sum_{j=1}^J \omega_{lj} f_1(\sum_{i=1}^I \omega_{ji} a_i - \theta_j) - \theta_l)]^2
 \end{aligned}
 \tag{3}$$

Where E is the overall error of output layer neurons; L is the number of neurons in output layer; t_i is the target value of output layer neuron.

D. Updating weights and biases

According to the error gradient descent method, the weights w_{ji} and ω_{lj} , the biases θ_j and θ_l can be updated by Equations 4 to 7.

$$\Delta \omega_{ji} = -\eta \frac{\partial E}{\partial \omega_{ji}}
 \tag{4}$$

$$\Delta \theta_j = -\eta \frac{\partial E}{\partial \theta_j}
 \tag{5}$$

$$\Delta \omega_{lj} = -\eta \frac{\partial E}{\partial \omega_{lj}}
 \tag{6}$$

$$\Delta \theta_l = -\eta \frac{\partial E}{\partial \theta_l}
 \tag{7}$$

Where Δw_{ji} is the update value of w_{ji} ; $\Delta \omega_{lj}$ is the update value of ω_{lj} ; $\Delta \theta_j$ is the update value of θ_j ; $\Delta \theta_l$ is the update value of θ_l ; η is the learning factor.

2.2 Particle Swarm Optimization

In PSO algorithm, the particle swarm searches the solution of problem in a D dimensional space, and the position of each particle is a solution of problem. Each particle searches new solutions by constantly adjusting its position. P_{best} is defined as the optimal solution of each moving particle, G_{best} is defined as the global optimal solution of the whole particle swarm, v is the velocity of each particle, x is the current location of each particle. Then, the particle's speed and position can be updated by Equations 8 and 9.

$$\begin{aligned}
 v_{id} &= \lambda \times v_{id} + u_1 \times r_1 \times (P_{best,d} - x_{id}) \\
 &+ u_2 \times r_2 \times (G_{best,d} - x_{id})
 \end{aligned}
 \tag{8}$$

$$x_{id} = x_{id} + v_{id}
 \tag{9}$$

Where, v_{id} is the d dimension velocity of particle i ; x_{id} is the d dimension position of particle i ; λ is the inertia weight; u_1 and u_2 are learning factors, which are also called acceleration constants, the learning factor controls the distance that a particle can move in a single iteration; r_1 and r_2 are uniform random number in $[0,1]$.

The inertia weight λ has great influence on the performance of PSO algorithm. When λ is too large, PSO algorithm can quickly converge to the global optimal solution, but it is easy to cause the fluctuation of the optimal solution. When λ is too small, PSO algorithm is easy to fall into the local optimal solution. Hence, in the paper, the inertia weight λ is calculated by Equation 10.

$$\lambda = \lambda_{max} - (\lambda_{max} - \lambda_{min}) \times \frac{n}{N}
 \tag{10}$$

Where, λ_{max} is the maximum inertia weight; λ_{min} is the minimum inertia weight; n is the current iteration number; N is the maximum iteration number.

In PSO algorithm, the fitness function describes the relationship between the current position of the particle and the optimal solution. In this paper, in order to reflect the relationship between the prediction value of PSO-BP neural network and the target value, the mean standard error (MSE) between the prediction value of BP neural network and the target value is selected as the fitness function, and the fitness function is shown as Equation 11.

$$Fit = \sqrt{\frac{\sum_{i=1}^k (p_i - q_i)^2}{k}}
 \tag{11}$$

Where, k is the number of training samples; p_i is the target value; q_i is the prediction value of PSO-BP neural network.

2.3 Proposed PSO-BP Neural Network

In the paper, the main idea of PSO-BP neural network is to use the global search ability of PSO algorithm to obtain the initial weights and biases of BP neural network, so as to overcome the problem that BP neural network is easy to fall into local optimal solution, and improve the convergence speed of BP neural network. The flow chart of the proposed PSO-BP neural network is shown in Figure 2.

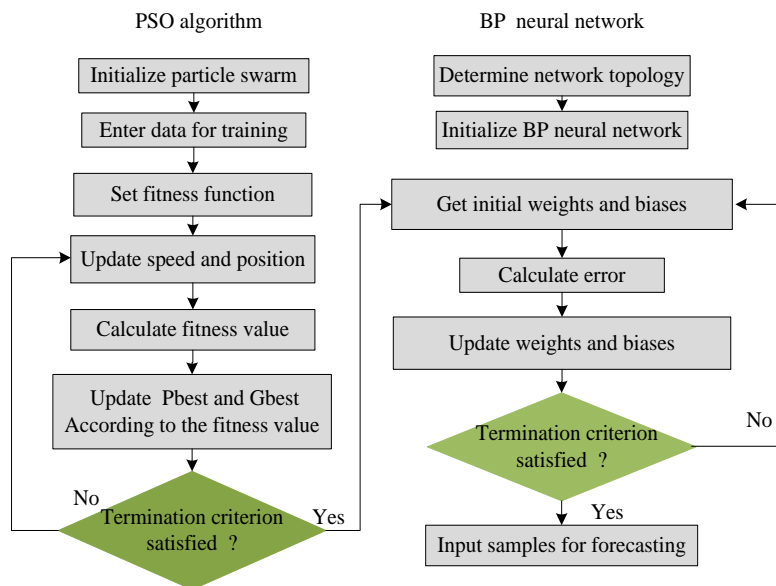


Fig. 2. Flow chart of PSO-BP neural network.

The calculation steps of PSO-BP neural network are as follows.

Step 1. Determine the neurons number I, J, L of the input layer, the hidden layer and the output layer of BP neural network respectively, and the learning factors η .

Step 2. Set the maximum velocity v_{max} and the minimum velocity v_{min} of particles, and randomly generate the velocity of particles within the region $[v_{max}, v_{min}]$.

Step 3. Randomly set the initial positions of particles, and the initial positions of the weights and biases of BP neural network.

Step 4. Initialize the inertia weight λ , learning factor u_1 and u_2 , the number M of particles, and the number N of iterations.

Step 5. Input training samples for calculating.

Step 6. Calculate the output of BP neural network, subsequently, calculate the fitness value of each particle according to Equation 11, and get the individual optimal solution P_{best} of each particle and the global optimal solution G_{best} of all the particles.

Step 7. Update particles' speed and positions according to Equations 8 and 9.

Step 8. Judge whether the maximum iterations number of PSO algorithm has been reached, if the maximum iterations number is not reached, loop back to step 6, otherwise, go to step 9.

Step 9. Get the optimal initial weights and biases of BP neural network from the global optimal solution G_{best} .

Step 10. Train BP neural network until the end condition is satisfied.

3. TRAINING PROCESS OF PSO-BP NEURAL NETWORK

3.1 Data Sources

The training data and testing data of the PSO-BP neural network are derived from a certain wind farm in northern China, and those data include wind tower data,

NWP data and the power output data of wind farm. The wind tower data and NWP data include wind speed, wind direction, temperature, humidity and air pressure, etc. The NWP data is calculated every 15 minutes, and the wind tower data and the power output data are acquired every 15 minutes. The wind tower data does not participate in the training process of PSO-BP neural network, which is mainly used to verify the correctness of NWP data. The wind farm has a total of 80 wind turbines, and the total power output of the wind farm is 120MW. The power curve of wind turbine is shown in Figure 3.

In order to make the training data include all the climatic conditions (including spring, summer, autumn and winter four seasons), the training data usually contain full 1 year data, or multi-years data. In this paper, the NWP data and power output data for PSO-BP neural network training is the full year data in 2011. The testing data are the NWP data and power output data of 6-h, 1-day, 3-day in May and December of 2012, respectively. The testing data are used to verify the superiority of PSO-BP neural networks under different forecasting time scales and different climatic conditions.

3.2 Training PSO-BP Neural Network

The 30540 groups NWP data in full year 2011 is used as the input of PSO-BP neural network, the actual power output of wind farm is selected as the target output, and the PSO-BP neural network is trained. Before training begins, the following parameters need to be determined.

a) Neuron number of the input layer in PSO-BP

The NWP data is used as the input of PSO-BP neural network, which contains the information of wind speed, wind direction, temperature, humidity, and air pressure. The wind direction information is described by the value of sine function and cosine function. Therefore, the number of input layer neuron of PSO-BP neural network is 6.

b) Neuron number of the hidden layer and the output layer in PSO-BP

According to the Kolmogorov theorem, the neuron number of hidden layer is 13. Because the output of PSO-BP neural network is the power output of wind farm, the neuron number of output layer is 1.

c) Set the parameters of PSO

In the paper, the particle number is 40; the learning factor u_1 and u_2 are set as 2; the maximum velocity v_{\max} and the minimum velocity v_{\min} of particles are set as 0.5 and 0.25, respectively; the maximum inertia weight λ_{\max} is set as 0.9 and the minimum inertia weight λ_{\min} is set as 0.3; the learning rate is set as 0.1.

d) End condition of PSO-BP Neural Network

The maximum iterative number of PSO is 200; the target error of BP is 0.00001; the learning rate of BP is 0.1; the maximum iterative number of BP is 100.

According to the above parameters setting, the PSO-BP neural network is trained. The change processes of the fitness function value of PSO is shown in Figure 4. It can be seen from Figure 4 that the fitness function value reaches a steady state when the number of iterations is about 90, and the calculation process is finished when the number of iterations reaches 200.

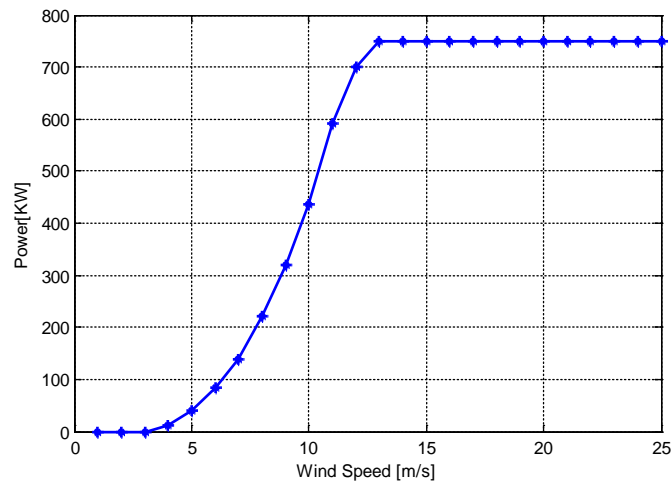


Fig. 3. Power curve of wind turbine.

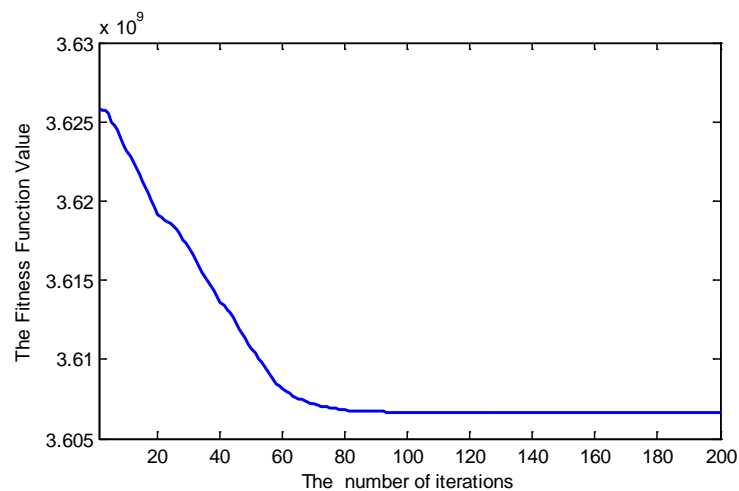


Fig. 4. Change processes of the fitness function value of PSO-BP.

4. WIND POWER FORECASTING

In order to verify that the PSO-BP neural network has good forecast ability in different climatic conditions and time scales, the trained PSO-BP neural network is used to forecast the power output of wind farm in 6 hours, 1 day and 3 days, from 0 o'clock on 28 December to 24 o'clock on 30 December, and from 8 o'clock on 17 May to 8 o'clock on 20 May, 2012. In order to verify the superiority of PSO-BP neural network, the prediction

results of original BP, PSO-BP, GA-BP and wavelet-BP neural network are compared and analyzed in the paper.

The mean absolute error (MAE) and the root mean square error (RMSE) are two very important indicators to evaluate the performance of the wind power forecasting. Therefore, the MAE and RMSE of original BP, PSO-BP, GA-BP and wavelet-BP neural network are compared and analyzed. The MAE and RMSE are calculated by Equations 12 and 13.

$$MAE = \left(\sum_{i=1}^N \left| \frac{t_i - c_i}{t_i} \right| \right) / N \tag{12}$$

$$RMSE = \sqrt{\left(\sum_{i=1}^N \left(\frac{t_i - c_i}{t_i} \right)^2 \right) / N} \tag{13}$$

Where N represents the number of testing samples; t_i represents target output; c_i represents forecasting output.

The wind speed data and NWP data from 0 o'clock on 28 December to 24 o'clock on 30 December, 2012 are shown in Figure 5. It can be seen from Figure 5 that the change process of NWP data is more gentle than that of wind tower data, mainly because the NWP data is obtained by numerical calculation based on the actual situation of the atmosphere, certain initial and boundary conditions. Therefore, there will be no significant change between the adjacent two points. However, for the wind speed data of wind tower, because of the impact of terrain, wind direction and wind turbines, the

wind speed data has certain random characteristics. But on the whole, the wind speed data and NWP data have the same trend, which is proved that the wind power forecasting based on NWP data is reasonable and feasible.

Figure 6 is the 6-h power forecasting from 0 o'clock to 6 o'clock on 28 December, 2012. It can be seen from Figure 6 that the forecasting power of original BP, PSO-BP, GA-BP and wavelet-BP have the same change trend with that of the actual power output of wind farm, which proves that these wind power forecast methods are correct and feasible for wind power forecasting. The MAE of wind power forecasting based on original BP, PSO-BP, GA-BP and wavelet-BP are 15.32%, 11.83%, 12.36% and 14.89%, respectively, and the RMSE based on original BP, PSO-BP, GA-BP and wavelet-BP are 17.09%, 16.41%, 16.86% and 17.32%, respectively. The forecasting results of MAE and RMSE show that the forecasting effect of PSO-BP neural network is better than that of original BP, GA-BP and wavelet-BP neural network.

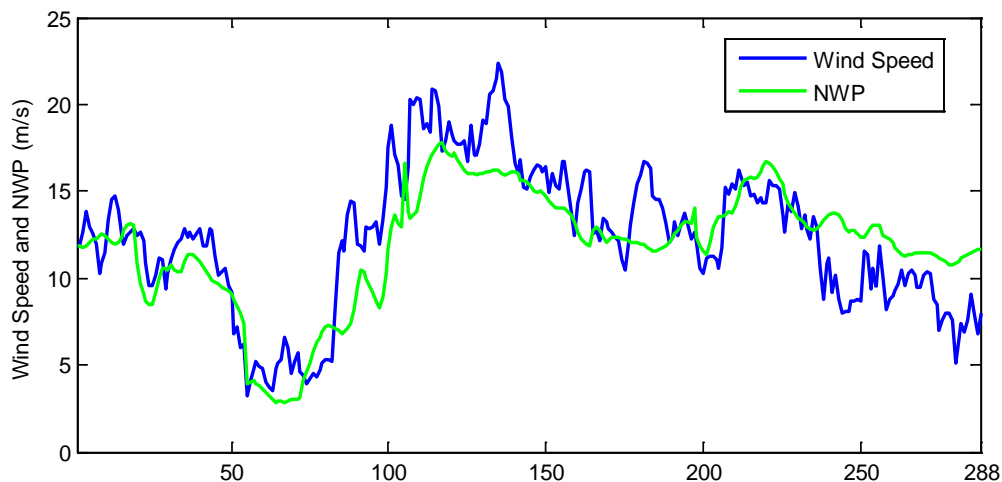


Fig. 5. Wind tower data and NWP data on December 28-30, 2012.

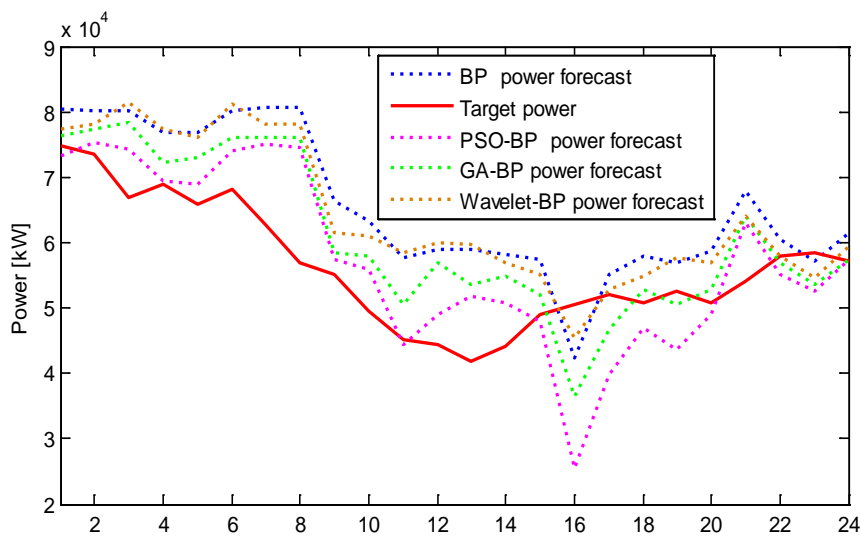


Fig. 6. 6-h power forecasting of December, 2012.

Table 1. MAE and RMSE based on BP, PSO-BP, GA-BP and wavelet-BP on December.

| Month | Time Scale of Forecasting | MAE | RMSE |
|-------|---------------------------|--------|--------|
| Dec. | 6-h of BP | 15.32% | 17.09% |
| | 6-h of PSO-BP | 11.83% | 16.41% |
| | 6-h of GA-BP | 12.36% | 16.86% |
| | 6-h of Wavelet-BP | 14.89% | 17.32% |
| | 1-day of BP | 25.28% | 31.00% |
| | 1-day of PSO-BP | 18.26% | 20.62% |
| | 1-day of GA-BP | 20.65% | 22.38% |
| | 1-day of Wavelet-BP | 23.34% | 25.87% |
| | 3-days of BP | 25.21% | 31.09% |
| | 3-days PSO-BP | 20.42% | 27.99% |
| | 3-days of GA-BP | 22.86% | 28.57% |
| | 3-days of Wavelet-BP | 24.65% | 29.94% |

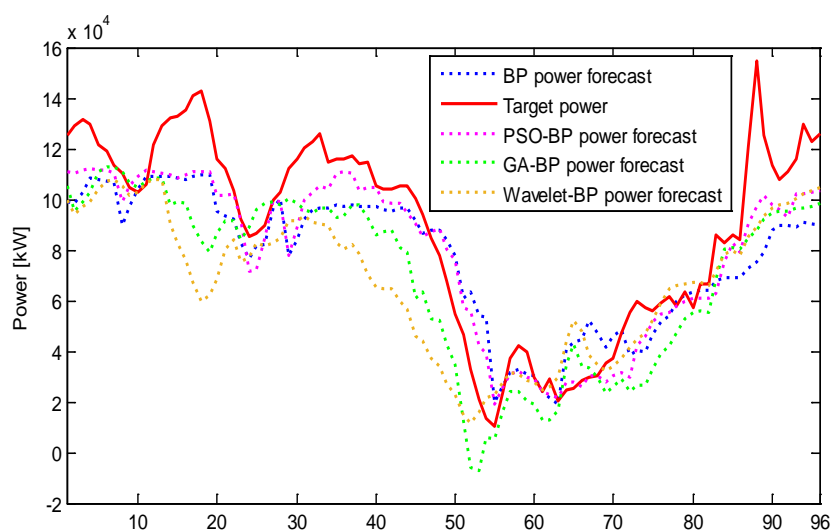
In order to verify that the PSO-BP neural network has better forecast effect in other time scales, the power output of wind farm are forecasted using the trained PSO-BP neural network from 0 o'clock to 24 o'clock on 28 December, 2012, and from 0 o'clock on 28 December to 0 o'clock on 30 December, 2012. The forecasting results are shown in Figure 7 and Figure 8. It can be seen from Figure 7 and Figure 8 that the forecasting power of original BP, PSO-BP, GA-BP, and wavelet-BP neural network has the same trend with the actual power output of wind farm.

For the forecasting results of 1-day, the MAE and RMSE of wind power forecasting based on PSO-BP neural network are 18.26% and 20.62%, the MAE and RMSE based on original BP are 25.28% and 31.00%, the MAE and RMSE based on GA-BP are 20.65% and 22.38%, and the MAE and RMSE based on wavelet-BP are 23.34% and 25.87%. For the forecasting results of 3-days, the MAE and RMSE based on PSO-BP are 20.42% and 27.99%, the MAE and RMSE based on original BP are 25.21% and 31.09%, the MAE and RMSE based on

GA-BP are 22.86% and 28.57%, and the MAE and RMSE based on wavelet-BP are 24.65% and 29.94%. For the time scale of 1-day and 3-days, the results of MAE and RMSE show that the prediction effect of PSO-BP neural network is still better than that of original BP, GA-BP and wavelet-BP neural network.

The MAE and RMSE based on original BP, PSO-BP, GA-BP, and wavelet-BP neural network under different time scales in December are shown in Table 1. It can be seen from Table 1 that the MAE and RMSE based on PSO-BP neural network are less than that based on original BP, GA-BP, and wavelet-BP neural network under different time scales.

In order to verify that the PSO-BP neural network still has good forecast ability in other climatic conditions, the power output of wind farm in 6-h, 1-day and 3-days, from 8 o'clock on 17 May to 8 o'clock on 20 May, 2012, is forecasted using the trained PSO-BP neural network. The wind speed data of wind tower and the NWP data on 17-20 May are shown in Figure 9. The forecasting results are shown in Figures 10, 11 and 12.

**Fig. 7. 1-day power forecasting of December 28, 2012.**

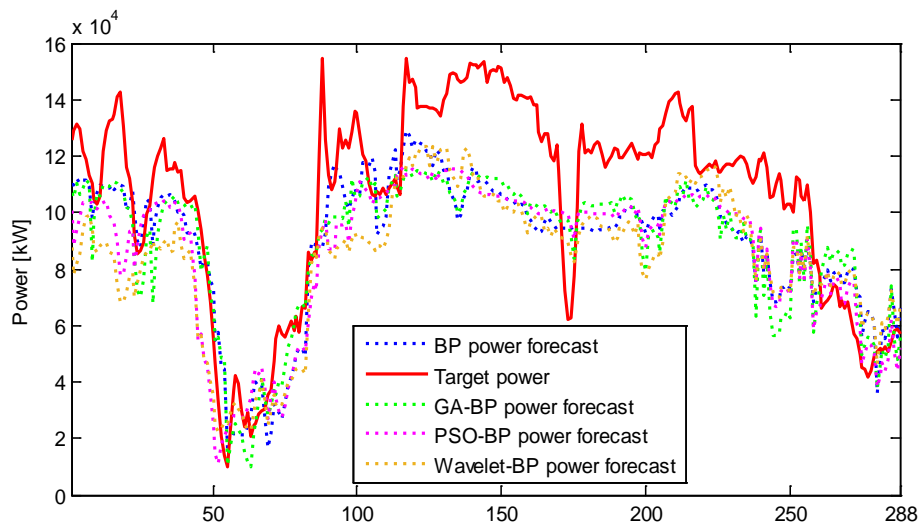


Fig. 8. 3-days power forecasting of December 28-30, 2012.

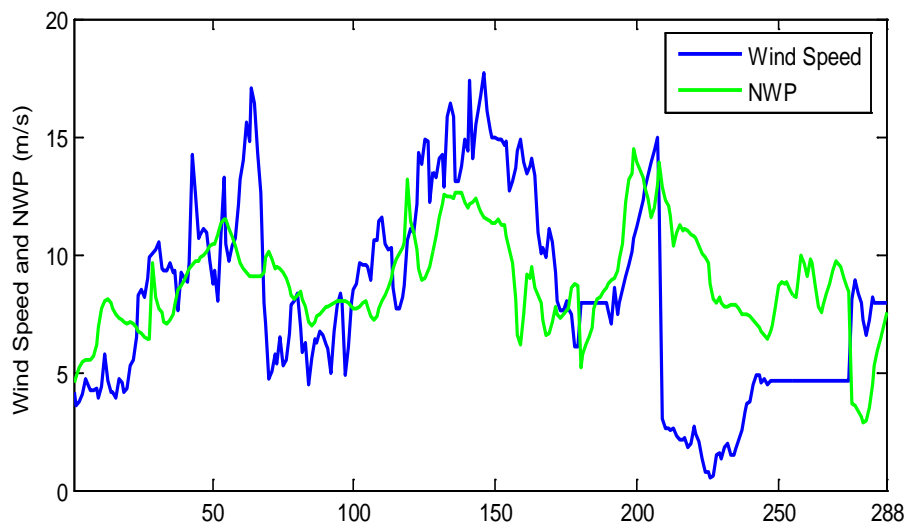


Fig. 9. Wind tower data and NWP data on May 17-20, 2012.

Figure 10 is the forecasting results of 6-h on May 17, 2012. The MAE and RMSE of the wind power forecasting based on PSO-BP neural network are 15.86% and 18.77%, the MAE and RMSE based on original BP are 17.58% and 20.62%, the MAE and RMSE based on GA-BP are 16.74% and 18.98%, and the MAE and RMSE based on wavelet-BP are 17.83% and 21.35%.

Figure 11 is the forecasting results of 1-day on 17 May, 2012. The MAE and RMSE based on PSO-BP neural network are 20.12% and 24.34%, the MAE and RMSE based on original BP are 24.32% and 22.64%, the MAE and RMSE based on GA-BP are 24.37% and 22.53%, and the MAE and RMSE based on wavelet-BP are 22.65% and 23.86%.

Figure 12 is the forecasting results of 3-day on May, 2012. The MAE and RMSE based on PSO-BP neural network are 23.55% and 26.79%, the MAE and RMSE based on original BP are 27.90% and 30.25%, the MAE and RMSE based on GA-BP are 24.47% and 27.89%, and the MAE and RMSE based on wavelet-BP are 26.76% and 29.38%.

It can be seen from Figures 10, 11 and 12 that the forecasting effect of PSO-BP neural network is still better than that of original BP, GA-BP and wavelet-BP neural network under different climatic conditions and time scales. It has been proven that the proposed PSO-BP neural network is reasonable and effective.

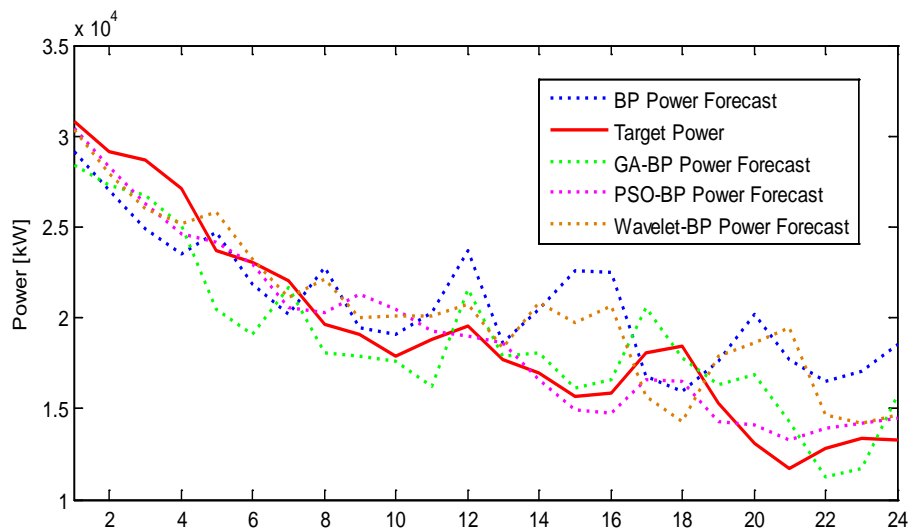


Fig. 10. 6-h power forecasting of May 17, 2012.

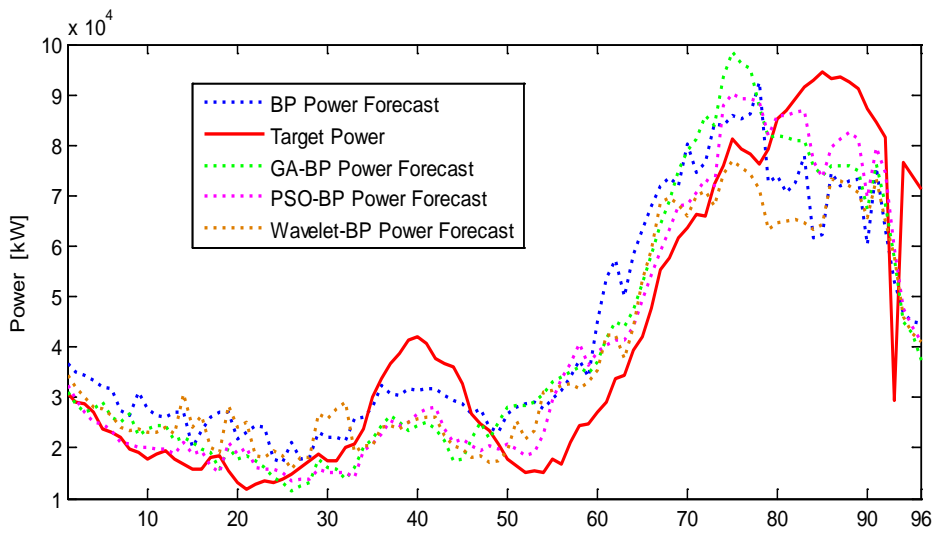


Fig. 11. 1-day power forecasting of May 17, 2012.

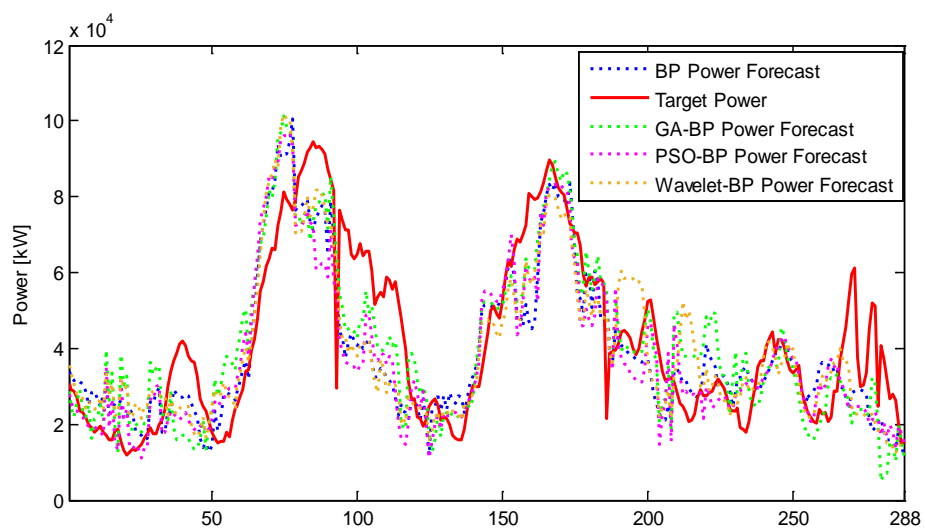


Fig. 12. 3-day power forecast of May 17-20, 2012.

The MAE and RMSE based on original BP, PSO-BP, GA-BP, and wavelet-BP neural network under different time scales in May are shown in Table 2. It can be seen from Table 2 that the MAE and RMSE based on

PSO-BP neural network are still less than that based on original BP, GA-BP, and wavelet-BP neural network under different time scales.

Figure 13 is a statistical chart of forecast error distribution, the statistical data is the forecast error of 3-day on 17-20 May, 2012. It can be seen from Figure 13 that the forecast error distribution of PSO-BP is mainly concentrated in the smaller numerical range, the forecast error of PSO-BP is less than 17,000 kW. However, for

BP, GA-BP, and wavelet-BP neural network, the forecast error still has a distribution between 17000 and 30000. The forecast error distributions of Figure 13 further confirm that the forecasting effect of PSO-BP neural network is still better than that of original BP, GA-BP and wavelet-BP neural network.

Table 2. MAE and RMSE based on BP, PSO-BP, GA-BP and wavelet-BP on May.

| Month | Time Scale of Forecasting | MAE | RMSE |
|-------|---------------------------|--------|--------|
| May | 6-h of BP | 17.58% | 20.62% |
| | 6-h of PSO-BP | 15.86% | 18.77% |
| | 6-h of GA-BP | 16.74% | 18.96% |
| | 6-h of Wavelet-BP | 17.83% | 21.35% |
| | 1-day of BP | 24.32% | 22.64% |
| | 1-day of PSO-BP | 20.12% | 24.34% |
| | 1-day of GA-BP | 21.37% | 22.53% |
| | 1-day of Wavelet-BP | 22.65% | 23.86% |
| | 3-days of BP | 27.90% | 30.25% |
| | 3-days PSO-BP | 23.55% | 26.79% |
| | 3-days of GA-BP | 24.47% | 27.89% |
| | 3-days of Wavelet-BP | 26.76% | 29.38% |

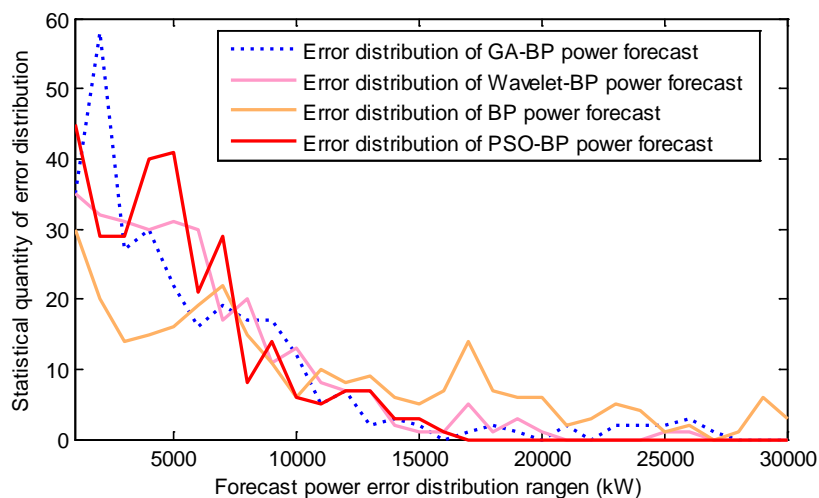


Fig. 13. statistical chart of forecast error distribution.

5. CONCLUSION

Considering the disadvantage of BP neural network forecasting method, a new wind power forecasting method based on PSO-BP neural network is proposed in the paper. This method uses the global search ability of PSO algorithm to obtain the initial weights and biases of BP neural network, which can effectively solve the problems of slow convergence speed and easy to fall into local optimal value of original BP algorithm.

The forecasting results of original BP, PSO-BP, GA-BP, and wavelet-BP neural network are compared and analyzed, and the comparison results show that the MAE and RMSE of wind power forecasting based on PSO-BP are less than that based on original BP, GA-BP,

and wavelet-BP neural network, which proves that the PSO-BP neural network is better than original BP, GA-BP, and wavelet-BP neural network in wind power forecasting.

ACKNOWLEDGEMENT

This study has been funded by the Key Projects of Science and Technology in Henan Province (152102210117), the Research Cooperation Project of Henan Province (162107000049), the Key Research Projects of Henan Higher Education Institutions (18A470004). Moreover, the authors wish to thank these people who have given a lot of help for the study, but their names are not listed in the paper.

REFERENCES

- [1] Arce M.P.D., Sauma E., and Contreras J., 2016. Renewable energy policy performance in reducing CO₂ emissions. *Energy Economics* 54: 272-280.
- [2] Scarlat N., Dallemand J.F., Monfortiferrario F., Banja M. and Motola V., 2015. Renewable energy policy framework and bioenergy contribution in the European Union - an overview from National Renewable Energy Action Plans and Progress Reports. *Renewable and Sustainable Energy Reviews* 51(6): 969-985.
- [3] Fais B., Sabio N., and Strachan N., 2016. The critical role of the industrial sector in reaching long-term emission reduction, energy efficiency and renewable targets. *Applied Energy* 162: 699-712.
- [4] Mathews A.P., 2014. Renewable energy technologies: panacea for world energy security and climate change. *Procedia Computer Science* 32: 731-737.
- [5] Jiang C., Liu W.X., Zhang J.H., Yu Y., Yu J.X., and Liu D.X., 2014. Risk assessment of power generation system with wind power access. *Transactions of China Electrotechnical Society* 29(2): 260-270.
- [6] Shi L., Luo Y., Tu G.Y., and Shi N., 2013. A method for preparing energy storage capacity considering the scheduling of wind farm. *Transactions of China Electrotechnical Society* 28(5): 120-127.
- [7] Soman S.S., Zareipour H., Malik O., and Mandal P., 2010. A review of wind power and wind speed forecasting methods with different time horizons. *North American Power Symposium*, Arlington, TX, USA, pp. 1-8.
- [8] Aggarwal S. and M. Gupta. 2013. Wind power forecasting: a review of statistical models. *International Journal of Science* 3: 1-10.
- [9] Gomes P. and R. Castro. 2012. Wind speed and wind power forecasting using statistical models: auto regressive moving average (ARMA) and artificial neural networks (ANN). *International Journal of Sustainable Energy* 1: 41-50.
- [10] Hering A.S. and M.G. Genton. 2012. Powering up with space-time wind forecasting. *Journal of American Statistical Association* 105(489): 92-104.
- [11] Wang X. and H. Li. 2012. Multi-scale prediction of wind speed and output power for the wind farm. *Journal of Control Theory and Application* 10(2): 251-258.
- [12] Dennis C.K., Asokan K., and Kumar K.S., 2016. Improved week-ahead predictions of wind speed using simple linear models with wavelet decomposition. *Renewable Energy* 93: 38-44.
- [13] Yan J. and K. Li. 2016. Time series wind power forecasting based on variant Gaussian Process and TLBO. *Neurocomputing* 189: 135-144.
- [14] Ding Z.Y., Yang P., Yang X., and Zhang Z., 2016. A wind power prediction method of support vector machine based on continuous time segment clustering. *Automation of Electric Power System* 36(14): 131-135.
- [15] Liu H., Tian H.Q., and Liang X.F., 2015. Wind speed forecasting approach using secondary decomposition algorithm and Elman neural networks. *Applied Energy* 157: 183-194.
- [16] Huang X.H., Li D.Y., and Lu G., 2011. wind speed prediction based on artificial neural network model. *Journal of Solar Energy* 32(2): 193-197.
- [17] Yang M.L., Liu S.M., and Wang Z.J., 2015. Calman wavelet neural network wind speed prediction. *Electric Power System and Automation* 27(10): 42-46.
- [18] Bonfil G.S., Ballesteros A.R., and Gershenson C., 2016. Wind speed forecasting for wind farms: A method based on support vector regression. *Renewable Energy* 85: 790-809.
- [19] Zeng Y.R., Zeng Y., Choi B., and Wang L., 2017. Multifactor-influenced energy consumption forecasting using enhanced back-propagation neural network. *Energy* 127: 381-396.
- [20] Wang Q., Li Y., Diao M., Gao W., and Qi Z., 2015. Performance enhancement of INS/CNS integration navigation system based on particle swarm optimization back propagation neural network. *Ocean Engineering* 108: 33-45.
- [21] Ren C., An N., Wang J.Z., Li L., Hu B., and Shang D., 2014. Optimal parameters selection for BP neural network based on particle swarm optimization: A case study of wind speed forecasting. *Knowledge Based Systems* 56: 226-239.
- [22] Pian Z.Y., Li S., Zhang H., and Zhang N., 2012. The application of the PSO based BP network in short-term load forecasting. *Physics Procedia* 24: 626-632.
- [23] Raza M.Q. and A. Khosravi. 2015. A review on artificial intelligence based load demand forecasting techniques for smart grid and buildings. *Renewable and Sustainable Energy Reviews* 50: 1352-1372.

